

Electronic Supplementary Information for

Infrared spectroscopy of $[\text{H}_2\text{O-X}_n]^+$ ($n = 1-3$, $X = \text{N}_2$, CO_2 , CO , and N_2O) radical cation clusters:

Competition between hydrogen bond and hemibond formation of the water radical cation

Department of Chemistry, Graduate School of Science, Tohoku University,

Sendai 980-8578, Japan

Mizuhiro Kominato and Asuka Fujii*

Contents

Fig. S1 Comparison of the observed IRPD and simulated anharmonic spectra of $[\text{H}_2\text{O-N}_2]^+\text{-Ar}$.

Fig. S2 Comparison of the observed IRPD and simulated spectra of $[\text{H}_2\text{O-N}_2]^+$.

Fig. S3 Comparison of the observed IRPD and simulated spectra of $[\text{H}_2\text{O-(N}_2)_2]^+$.

Fig. S4 Comparison of the observed IRPD and simulated spectra of $[\text{H}_2\text{O-(N}_2)_3]^+$.

Fig. S5 Comparison of the observed IRPD and simulated anharmonic spectra of $[\text{H}_2\text{O-CO}_2]^+\text{-Ar}$.

Fig. S6 Comparison of the observed IRPD and simulated spectra of $[\text{H}_2\text{O-CO}_2]^+$.

Fig. S7 Comparison of the observed IRPD and simulated spectra of $[\text{H}_2\text{O-(CO}_2)_2]^+$.

Fig. S8 Comparison of the observed IRPD and simulated spectra of $[\text{H}_2\text{O-(CO}_2)_3]^+$.

Fig. S9 Comparison of the observed IRPD and simulated anharmonic spectra of $[\text{H}_2\text{O-CO}]^+\text{-Ar}$.

Fig. S10 Comparison of the observed IRPD and simulated spectra of $[\text{H}_2\text{O-(CO)}_2]^+$.

Fig. S11 Comparison of the observed IRPD and simulated spectra of $[\text{H}_2\text{O-(CO)}_3]^+$.

Fig. S12 Observed IRPD spectrum of $[\text{H}_2\text{O-(CO)}_4]^+$.

Fig. S13 Comparison of the observed IRPD and simulated anharmonic spectra of $[\text{H}_2\text{O-N}_2\text{O}]^+\text{-Ar}$.

Fig. S14 Comparison of the observed IRPD and simulated spectra of $[\text{H}_2\text{O-N}_2\text{O}]^+$.

Fig. S15 Comparison of the observed IRPD and simulated spectra of $[\text{H}_2\text{O-(N}_2\text{O)}_2]^+$.

Fig. S16 Comparison of the observed IRPD and simulated spectra of $[\text{H}_2\text{O-(N}_2\text{O)}_3]^+$.

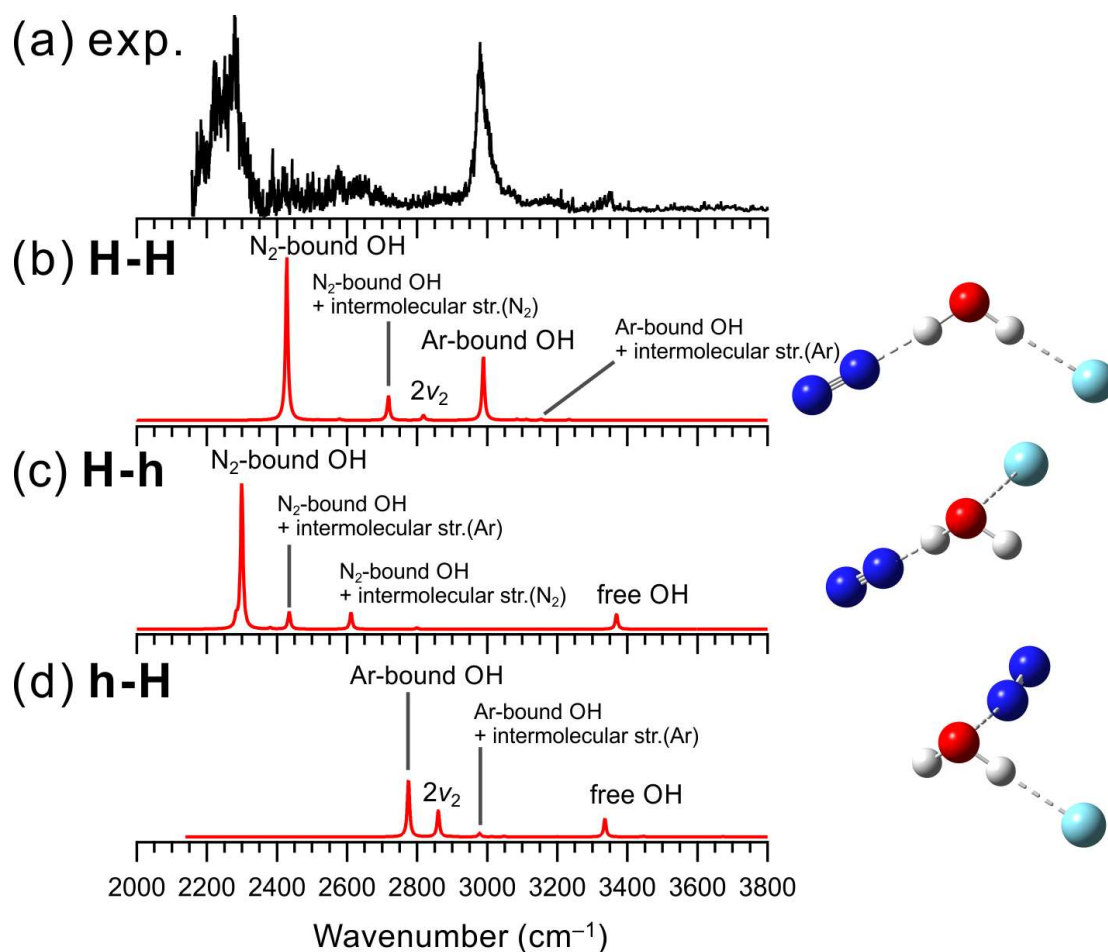


Fig. S1 Comparison of (a) observed IRPD spectrum of $[\text{H}_2\text{O-N}_2]^+\text{-Ar}$ and (b-d) simulated anharmonic (VPT2) spectra of the stable isomers calculated at MP2/aug-cc-pVTZ. The intensities of the simulated spectra of the isomers are plotted in the same scale. The schematic structures of the isomers are also shown.

The peaks at 2250, 2600, 2990, and 3160 cm^{-1} in the observed spectrum can be attributed to the N_2 -bound OH stretching, its combination band with the intermolecular stretching vibration, Ar-bound OH stretching, and its combination band with the intermolecular stretching vibration, respectively. The anharmonic calculational results show that the most stable structure, isomer **H-H**, well reproduces the observed features including the minor combination bands. Therefore, isomer **H-H** is assigned to the major carrier of the observed spectrum (see main text for details).

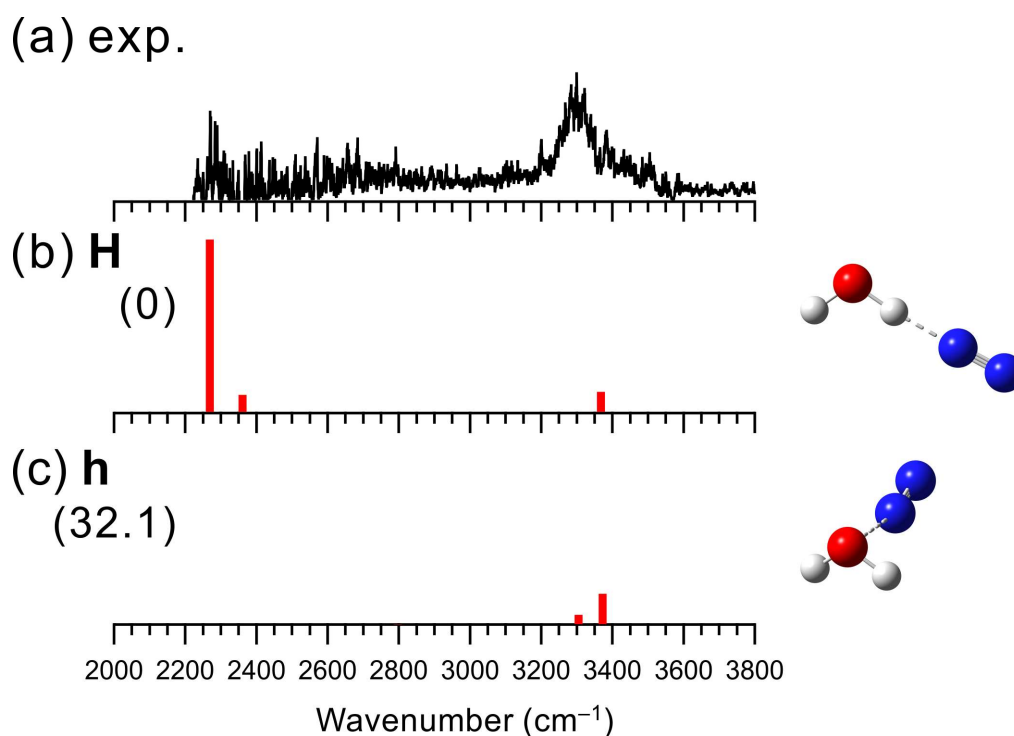


Fig. S2 Comparison of (a) observed IRPD spectrum of $[\text{H}_2\text{O-N}_2]^+$ and (b, c) simulated spectra of the stable isomers calculated at MP2/aug-cc-pVTZ. The simulated spectra were scaled by a factor of 0.955. The intensities of the simulated spectra of the isomers are plotted in the same scale. The schematic structures of the isomers are also shown. Numbers in parentheses are ZPE-corrected relative energies (in kJ/mol).

The peak at 3300 cm^{-1} and weak shoulders around 3420 cm^{-1} in the observed spectrum can be attributed to the symmetric (ν_1) and asymmetric (ν_3) free OH stretching vibrations of the hemibonded type isomer (**h**), respectively. The band features in the observed spectrum are quite similar to those of the previously reported IR spectrum of $[\text{H}_2\text{O-Kr}]^+$,¹ which also has a hemibonded structure. In the spectrum of $[\text{H}_2\text{O-Kr}]^+$, the broadening of the ν_3 band is attributed to the rotational structure. In the observed spectrum of $[\text{H}_2\text{O-N}_2]^+$, the H-bonded OH stretching band of the H-bonded type isomer (**H**) is totally absent. This suggests that isomer **h**, which does not have H-bonded OH, is the major isomer.

On the other hand, isomer **H** is calculated to be 32.1 kJ/mol more stable than isomer **h**.

Therefore, the theoretical results seem inconsistent with the experimental observation. Here, we should note the binding energy of each isomer. The MP2/aug-cc-pVTZ level was employed for the computations. The binding energies with the ZPE corrections were calculated to be 4657 and 1974 cm^{-1} for isomers **H** and **h**, respectively. These values indicate that isomer **H** cannot be dissociated with the IR photon absorption in the observed frequency range, while isomer **h** can be dissociated. Therefore, bands due to the major isomer (**H**) are missing in the observed spectrum, and only the bands of the minor isomer (**h**) appear. The fragment intensity detected in the IR spectral measurement was much weaker than that in the measurements of $n \geq 2$ clusters, as seen in the much poorer signal-to-noise (S/N) ratio of the present spectrum. This also supports the above-described scenario.

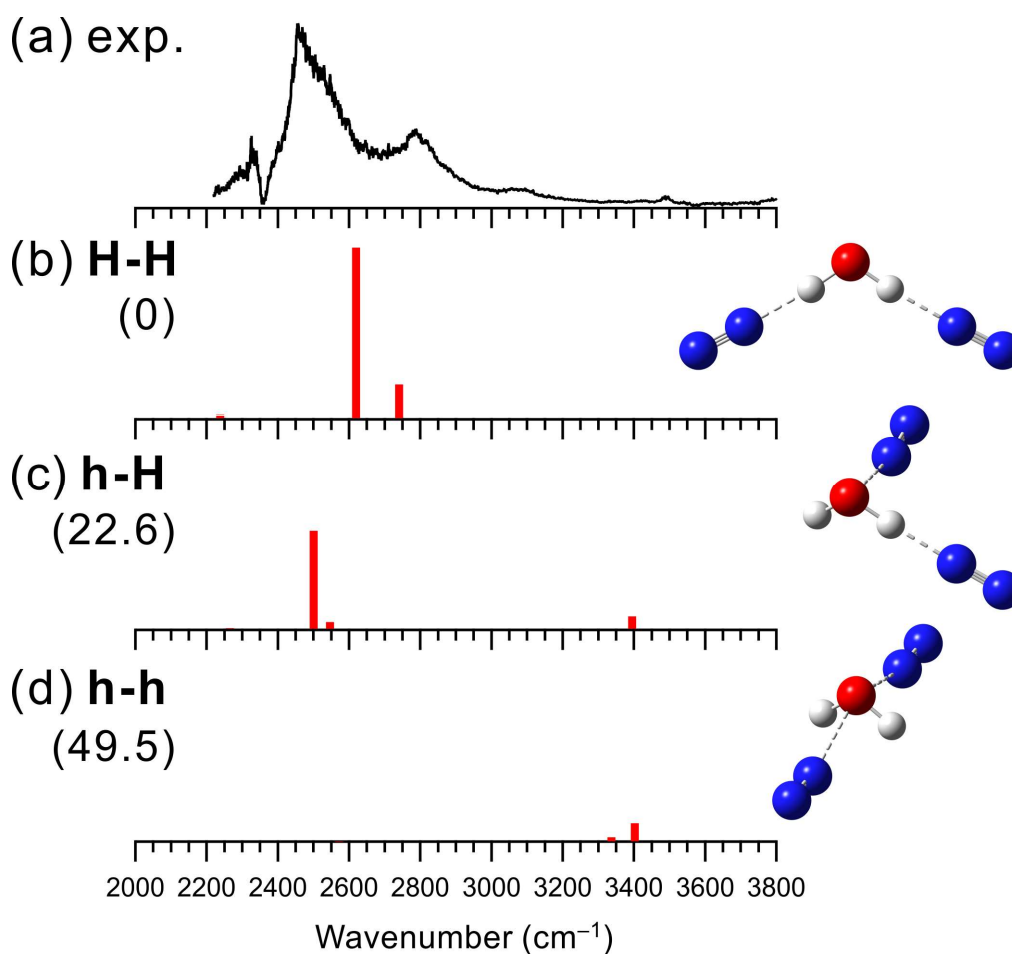


Fig. S3 Comparison of (a) observed IRPD spectrum of $[\text{H}_2\text{O}-(\text{N}_2)_2]^+$ and (b-d) simulated spectra of the stable isomers calculated at MP2/aug-cc-pVTZ. The simulated spectra were scaled by a factor of 0.955. The intensities of the simulated spectra of the isomers are plotted in the same scale. The schematic structures of the isomers are also shown. Numbers in parentheses are ZPE-corrected relative energies (in kJ/mol).

The peaks at 2330, 2470, and 2780 cm^{-1} in the observed spectrum can be attributed to the N_2 stretching, N_2 -bound OH stretching, and its combination band with intermolecular stretching vibration, respectively. Though the N_2 stretching band is forbidden in bare N_2 , its weak appearance is predicted in the simulations of the cluster. The two predicted bands of the N_2 -bound OH stretching vibrations may not be resolved in the observed spectrum. The combination band cannot be predicted in the present harmonic calculations. As no remarkable bands were observed in the free OH stretching

vibrational region, it is concluded that the observed structure is isomer **H-H**, which is calculated to be the most stable one. This means that the H-bond formation is preferred over the hemibond formation for $X = N_2$. The weak peak at 3500 cm^{-1} in the observed spectrum could be attributed to the minor population of isomer **h-H**. The coexistence of a little isomer **h-H** is consistent with the observation of the hemibonded isomer (**h**) at $n = 1$.

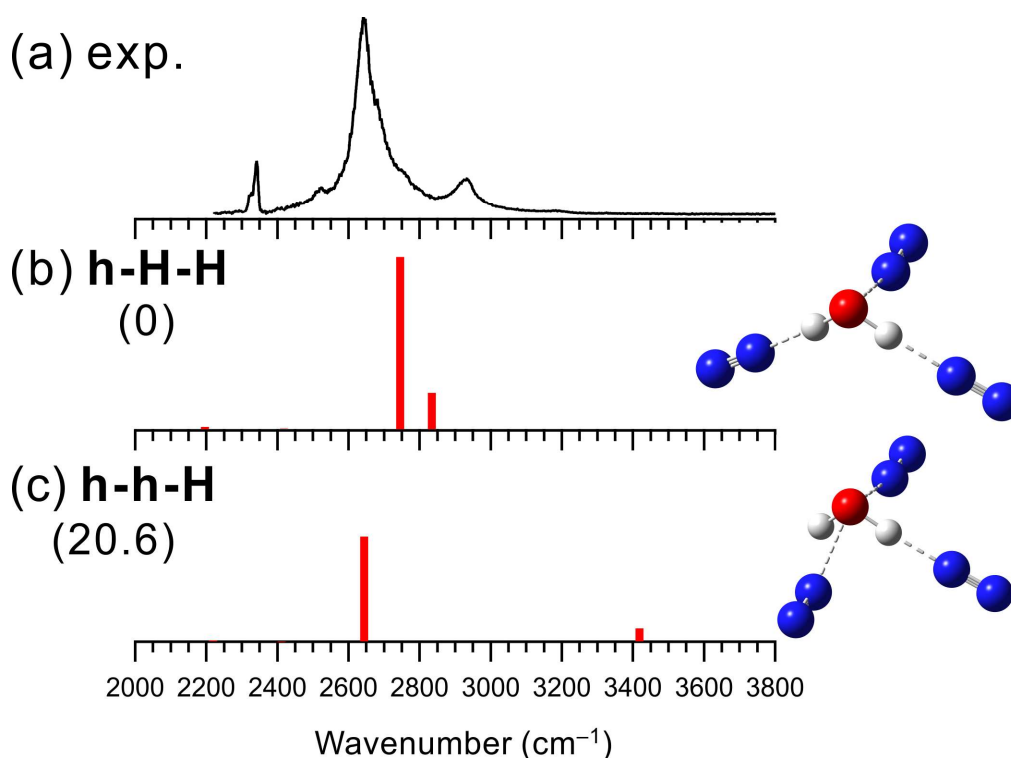


Fig. S4 Comparison of (a) observed IRPD spectrum of $[\text{H}_2\text{O}-(\text{N}_2)_3]^+$ and (b, c) simulated spectra of the stable isomers calculated at MP2/aug-cc-pVTZ. The simulated spectra were scaled by a factor of 0.955. The intensities of the simulated spectra of the isomers are plotted in the same scale. The schematic structures of the isomers are also shown. Numbers in parentheses are ZPE-corrected relative energies (in kJ/mol).

The peaks at 2340, 2640, and 2930 cm^{-1} in the observed spectrum can be attributed to the N_2 stretching, N_2 -bound OH stretching, and its combination band with intermolecular stretching vibration, respectively. It is noted that there are no bands in the free OH stretching vibrational region. Therefore, this spectrum is uniquely attributed to isomer **h-H-H**, in which the two N_2 molecules are H-bonded to the two OH groups and the third molecule is hemibonded to the O atom of H_2O^+ . Isomer **h-H-H** is the most stable isomer, and its predominant population is consistent with the observation. Though the H-bond formation is superior to the hemibond formation for $X = \text{N}_2$, both the H-bond donor sites (the OH groups) are occupied in $n = 2$, and then the third N_2 molecule is bound to the O atom of H_2O^+ with the hemibond. Isomer **h-H-H** demonstrates that the hemibond between H_2O^+ and

N_2 is stable even though it is weaker than the H-bonds.

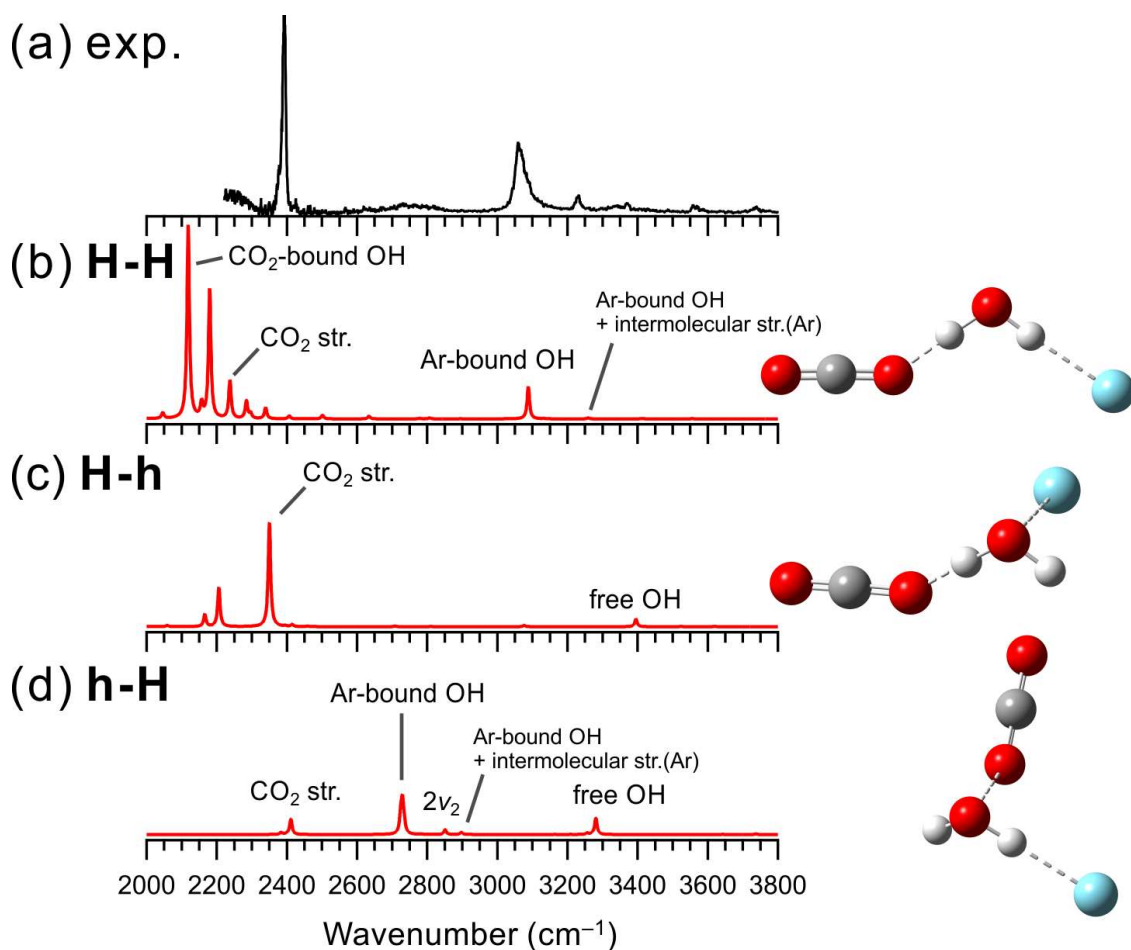


Fig. S5 Comparison of (a) observed IRPD spectrum of $[\text{H}_2\text{O-CO}_2]^+-\text{Ar}$ and (b-d) simulated anharmonic (VPT2) spectra of the stable isomers calculated at MP2/aug-cc-pVTZ. The intensities of the simulated spectra of the isomers are plotted in the same scale. The schematic structures of the isomers are also shown.

The peaks at 2390, 3070, and 3230 cm^{-1} in the observed spectrum can be attributed to the CO₂ stretching, Ar-bound OH stretching, and its combination band with the intermolecular stretching vibration, respectively. The anharmonic calculational results show that the most stable structure, isomer **H-H**, well reproduces the observed features including the combination band. Therefore, isomer **H-H** is assigned to the major carrier of the observed spectrum (see main text for details).

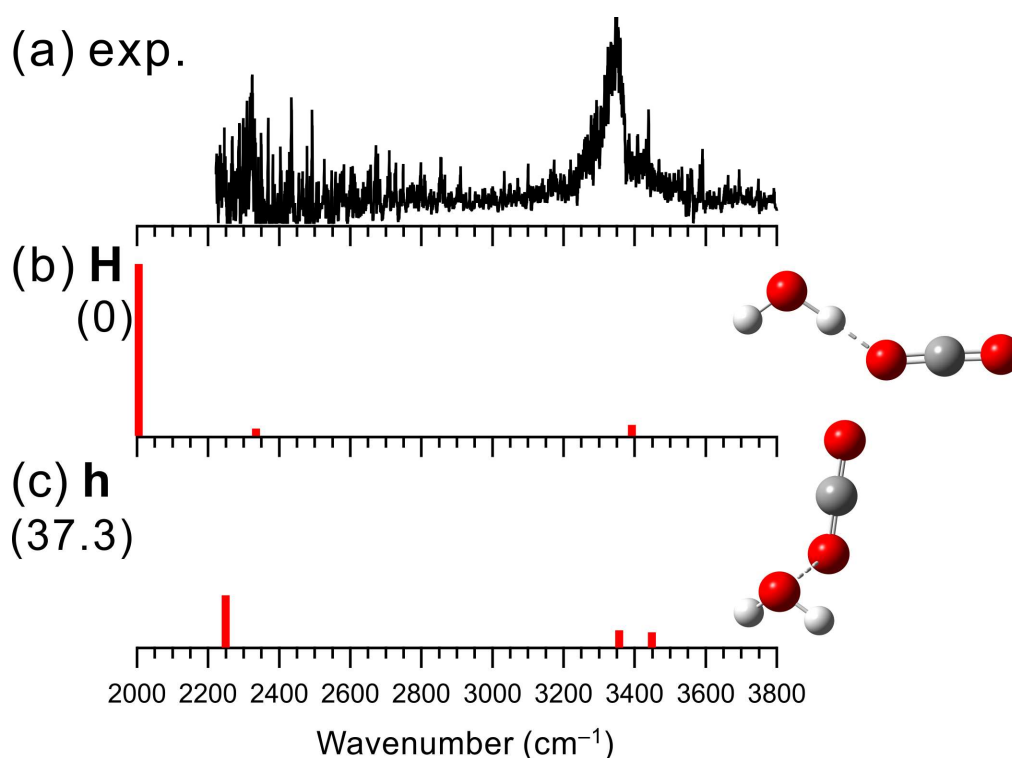


Fig. S6 Comparison of (a) observed IRPD spectrum of $[\text{H}_2\text{O}-\text{CO}_2]^+$ and (b, c) simulated spectra of the stable isomers calculated at MP2/aug-cc-pVTZ. The simulated spectra were scaled by a factor of 0.955. The intensities of the simulated spectra of the isomers are plotted in the same scale. The schematic structures of the isomers are also shown. Numbers in parentheses are ZPE-corrected relative energies (in kJ/mol).

The spectral features are similar to those of $[\text{H}_2\text{O}-\text{N}_2]^+$ (Fig. S2). The band at 3340 cm^{-1} and the small shoulders around 3400 cm^{-1} can be attributed to the symmetric (ν_1) and asymmetric (ν_3) free OH stretching vibrations of the hemibonded isomer (**h**), respectively. An experimental IR spectrum attributed to isomer **H** has been reported by Inokuchi *et al.*,² and a free OH stretch band appears at 3520 cm^{-1} , which is clearly different from the present spectrum. This also supports that isomer **h** is observed in the present measurement. Isomer **h** is calculated to be 37.3 kJ/mol less stable than isomer **H**, and such missing of the most stable isomer in the observed spectrum is also found in the case of $[\text{H}_2\text{O}-\text{N}_2]^+$. The missing of isomer **H** can be explained in terms of its high binding energy. The binding energies with the ZPE corrections were calculated (MP2/aug-cc-pVTZ) to be 7028 cm^{-1} and 3908

cm^{-1} for isomers **H** and **h**, respectively. Therefore, isomer **H** cannot be dissociated in the present IR predissociation measurement, and only minor isomer **h** would be observed with the help of some internal energy. Because of the weak fragment signal, the S/N ratio of the observed spectrum is poor. This supports that only the minor isomer could contribute to the observed spectrum.

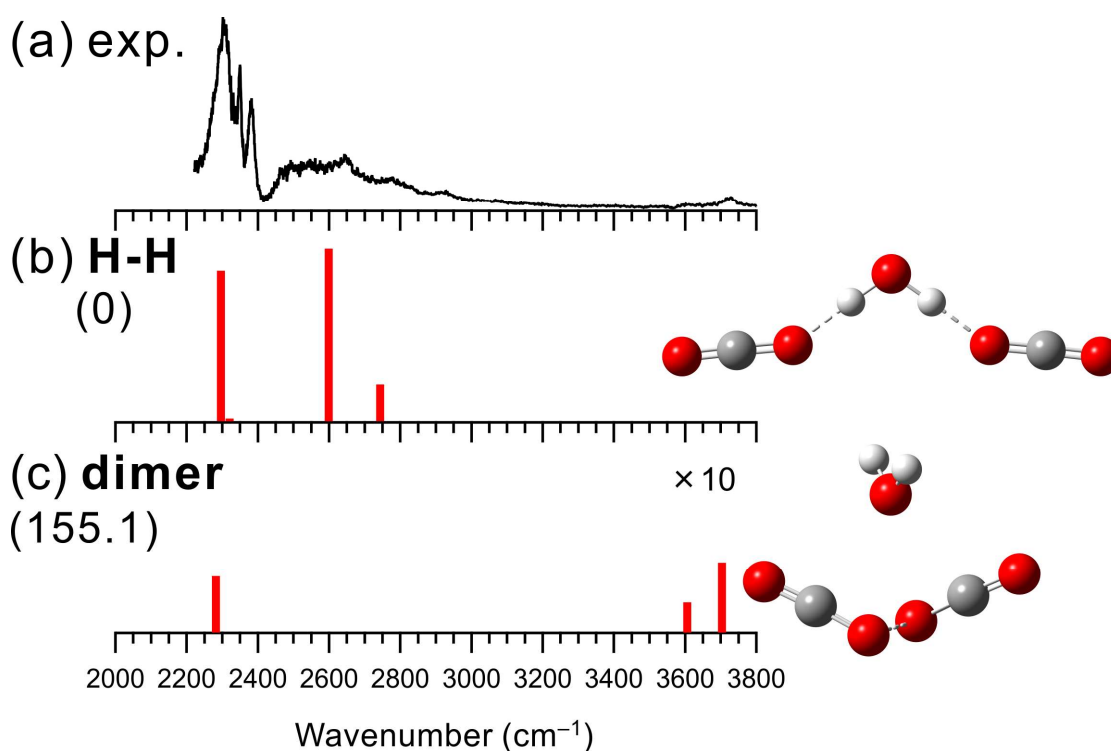


Fig. S7 Comparison of (a) observed IRPD spectrum of $[\text{H}_2\text{O}-(\text{CO}_2)_2]^+$ and (b, c) simulated spectra of the stable isomers calculated at MP2/aug-cc-pVTZ. The simulated spectra were scaled by a factor of 0.955. The intensities of the simulated spectra of the isomers are plotted in the same scale. The schematic structures of the isomers are also shown. Numbers in parentheses are ZPE-corrected relative energies (in kJ/mol).

The observed spectrum is essentially the same as that previously reported by Inokuchi *et al.*² The peaks around 2300 cm^{-1} and 2600 cm^{-1} in the observed spectrum can be assigned to the asymmetric CO stretching vibrations of the two CO_2 molecules and the CO_2 -bound OH stretching vibrations, respectively. In addition, the bands around 3600 and 3720 cm^{-1} are attributed to the $\nu_1 + \nu_3$ and $2\nu_2 + \nu_3$ combination bands of CO_2 , respectively, as reported by Inokuchi *et al.*² Here, ν_1 , ν_2 , and ν_3 represent the symmetric stretching, bending, and asymmetric stretching vibrations of CO_2 . These two combination bands are not calculated in the simulated spectrum under the harmonic approximation. As no clear free OH stretching vibrational bands are observed, the observed spectrum is attributed to isomer **H-H**, which is calculated to be the most stable isomer of $n = 2$, as has been demonstrated by

Inokuchi *et al.*² In the previous study by Inokuchi *et al.*, a characteristic band was observed at ~ 2030 cm^{-1} , which is assigned to the CO stretching vibration of the $(\text{CO}_2)_2^+$ dimer ion core of isomer **dimer**. Although the coexistence of a little isomer **dimer** is not excluded in the present study, we could not perform reliable measurements in the region below 2200 cm^{-1} because of the weak IR light power.

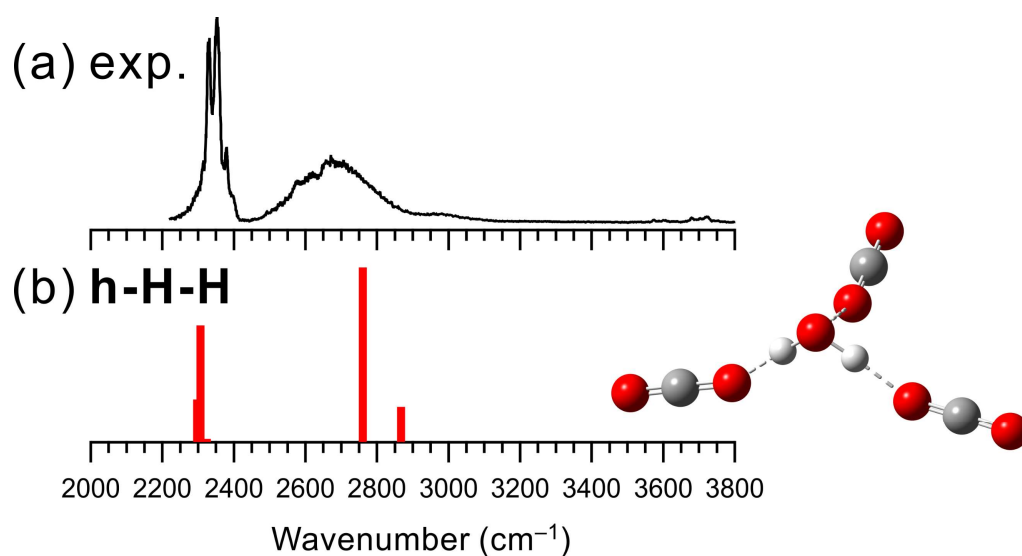


Fig. S8 Comparison of (a) observed IRPD spectrum of $[\text{H}_2\text{O}-(\text{CO}_2)_3]^+$ and (b) simulated spectrum of the stable isomer calculated at MP2/aug-cc-pVTZ. The simulated spectrum was scaled by a factor of 0.955. The schematic structure of the isomer is also shown.

Isomer (**h-H-H**) was obtained as a unique stable isomer at $n = 3$. The peaks at 2330 and 2360 cm^{-1} in the observed spectrum can be attributed to the asymmetric CO stretching vibrations of the hemibonded CO_2 and H-bonded CO_2 moieties, respectively. In addition, the band around 2700, 3600, and 3700 cm^{-1} are assigned to the CO_2 -bound OH stretching vibrations, $\nu_1 + \nu_3$, and $2\nu_2 + \nu_3$ combination bands of CO_2 , respectively, as shown in the previous study by Inokuchi *et al.*²

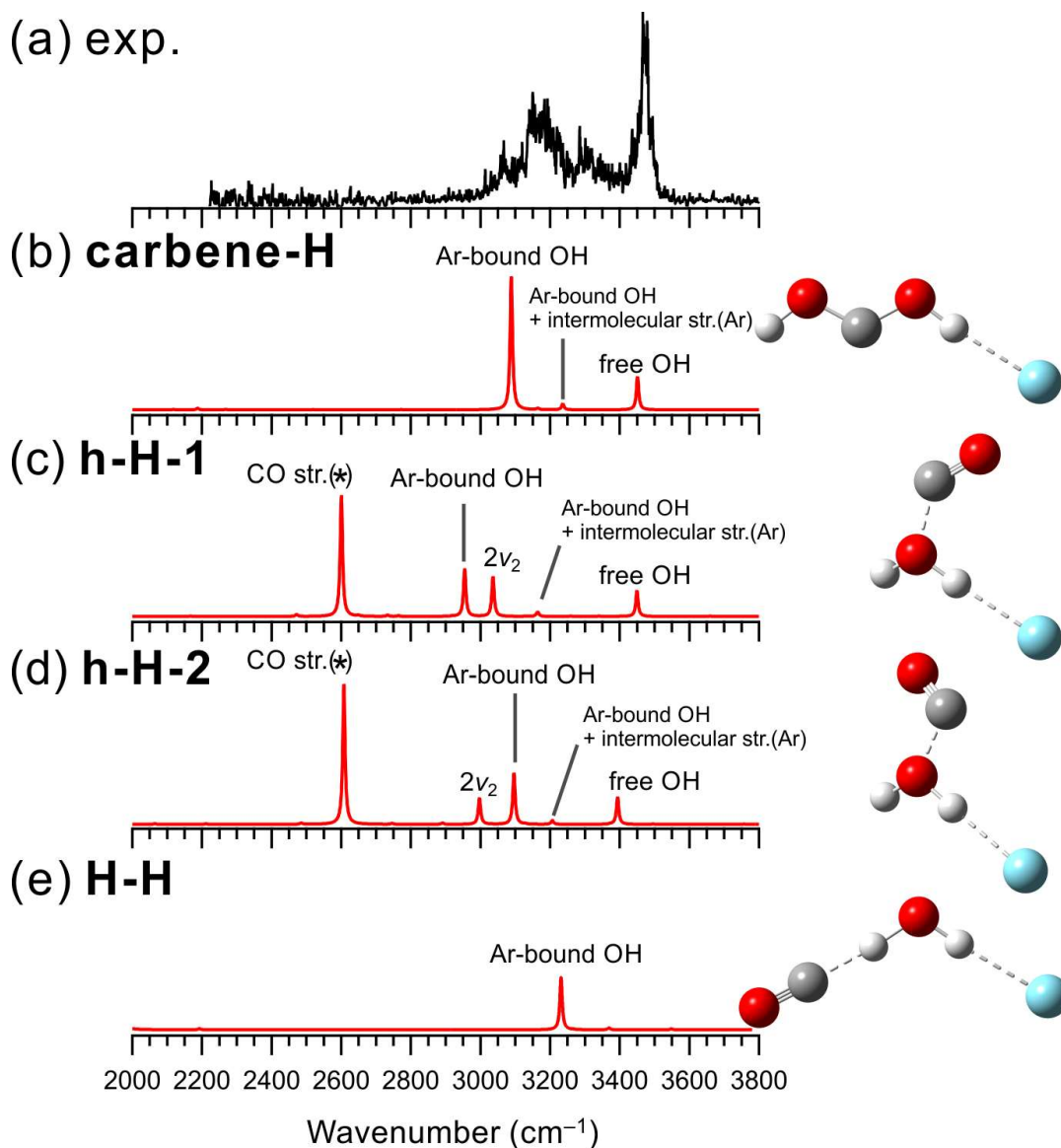


Fig. S9 Comparison of (a) observed IRPD spectrum of $[\text{H}_2\text{O-CO}]^+\text{-Ar}$ and (b-e) simulated anharmonic (VPT2) spectra of the stable isomers calculated at MP2/aug-cc-pVTZ. The intensities of the simulated spectra of the isomers are plotted in the same scale. The schematic structures of the isomers are also shown. In calculated spectra (c) and (d), the frequency of CO stretching vibration marked with the asterisk could be overestimated with the MP2 calculation (see main text for detail.)

The carbene-type isomer (**carbene-H**) is much more stable than the hemibonded type (**h-H-1** and **h-H-2**). However, the isomerization to the carbene form is unlikely to occur because the isomerization barrier is calculated to be quite high (~ 170 kJ/mol),^{3,4} and the isomerization seems

unlikely to fully occur. Anharmonic calculations show that both carbene-type and hemibonded isomers exhibit similar vibrational bands: Ar-bound OH stretching, its combination, and free OH stretching band. A notable difference between the spectra of the two structural motifs is the bending overtone band of H_2O^+ ($2\nu_2$). For isomer **carbene-H**, only the Ar-bound OH stretching band is predicted in the 3000-3200 cm^{-1} region, while for the hemibonded isomers, a water bending overtone is calculated in this region in addition to the Ar-bound OH stretching band (the Fermi resonance occurs). Therefore, the calculated spectra of the hemibonded isomers well reproduce the observed spectrum, especially, the shoulder band around 3070 cm^{-1} . We concluded that the coexistence of the carbene-type and hemibonded isomers are plausible (see main text for details).

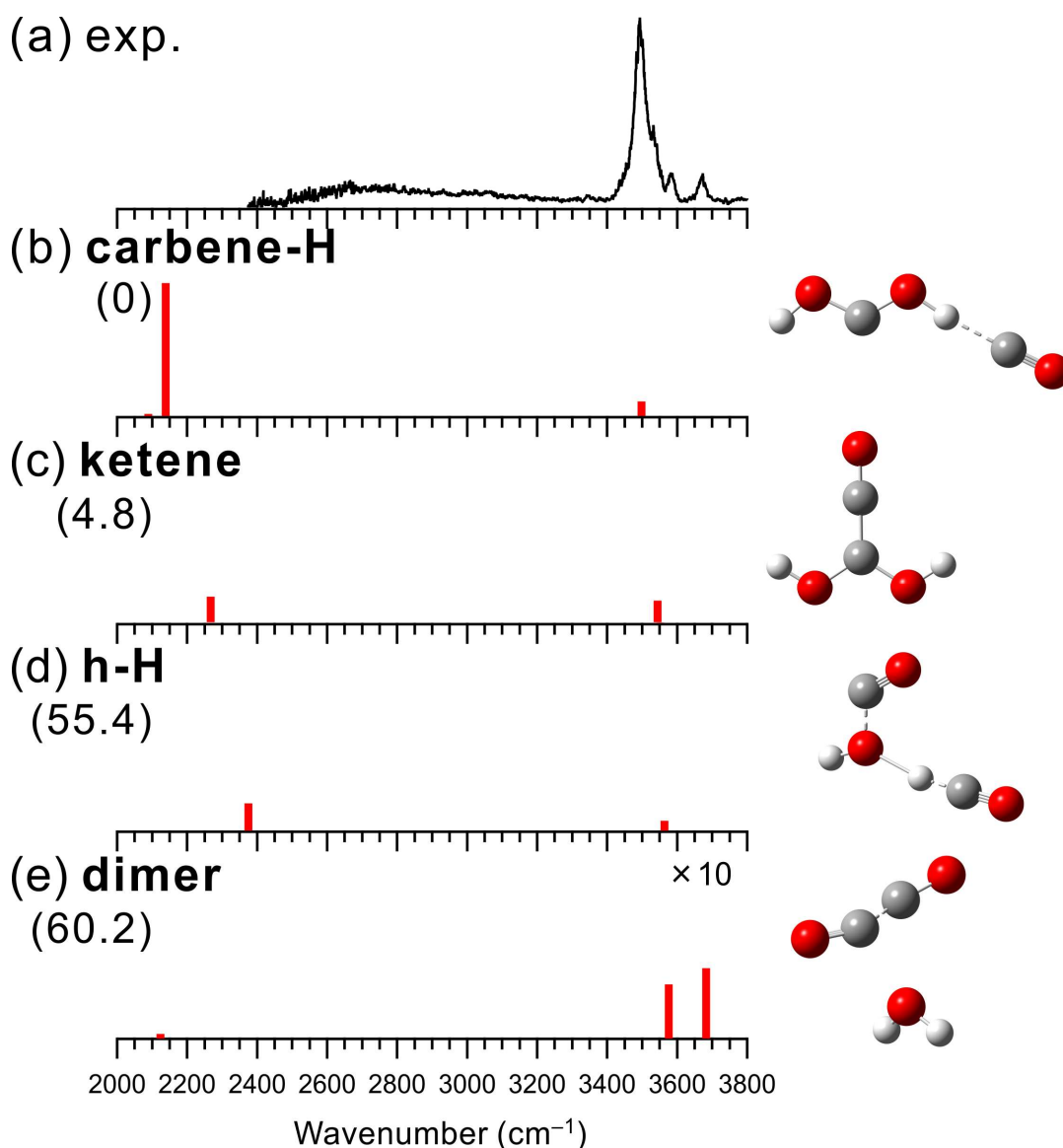


Fig. S10 Comparison of (a) observed IRPD spectrum of $[\text{H}_2\text{O}-(\text{CO})_2]^+$ and (b-e) simulated spectra of the stable isomers calculated at MP2/aug-cc-pVTZ. The simulated spectra were scaled by a factor of 0.955. The intensities of the simulated spectra of the isomers are plotted in the same scale. The schematic structures of the isomers are also shown. Numbers in parentheses are ZPE-corrected relative energies (in kJ/mol).

The peak at 3490 cm^{-1} in the observed spectrum can be attributed to a free OH stretching vibration. However, since most isomers are expected to show a band around 3500 cm^{-1} , the observed isomer structure cannot be uniquely determined by the comparison with the spectral simulations. The

previous study by Wong *et al.* has shown that the isomerization barrier to the carbene form is much lower in $n \geq 2$ (~ 0.8 kJ/mol) than that in $n = 1$ (~ 170 kJ/mol).⁴ Therefore, the most stable isomer (**carbene-H**) could be predominantly formed. On the other hand, the bands at 3580 cm^{-1} and 3670 cm^{-1} in the observed spectrum can be attributed to the ν_1 and ν_3 vibrations of neutral H_2O , respectively. These bands cannot be attributed to the carbene, ketene, or hemibonded forms. Therefore, they would be contributions of the CO dimer core type isomer (**dimer**), although this isomer is energetically very unstable.

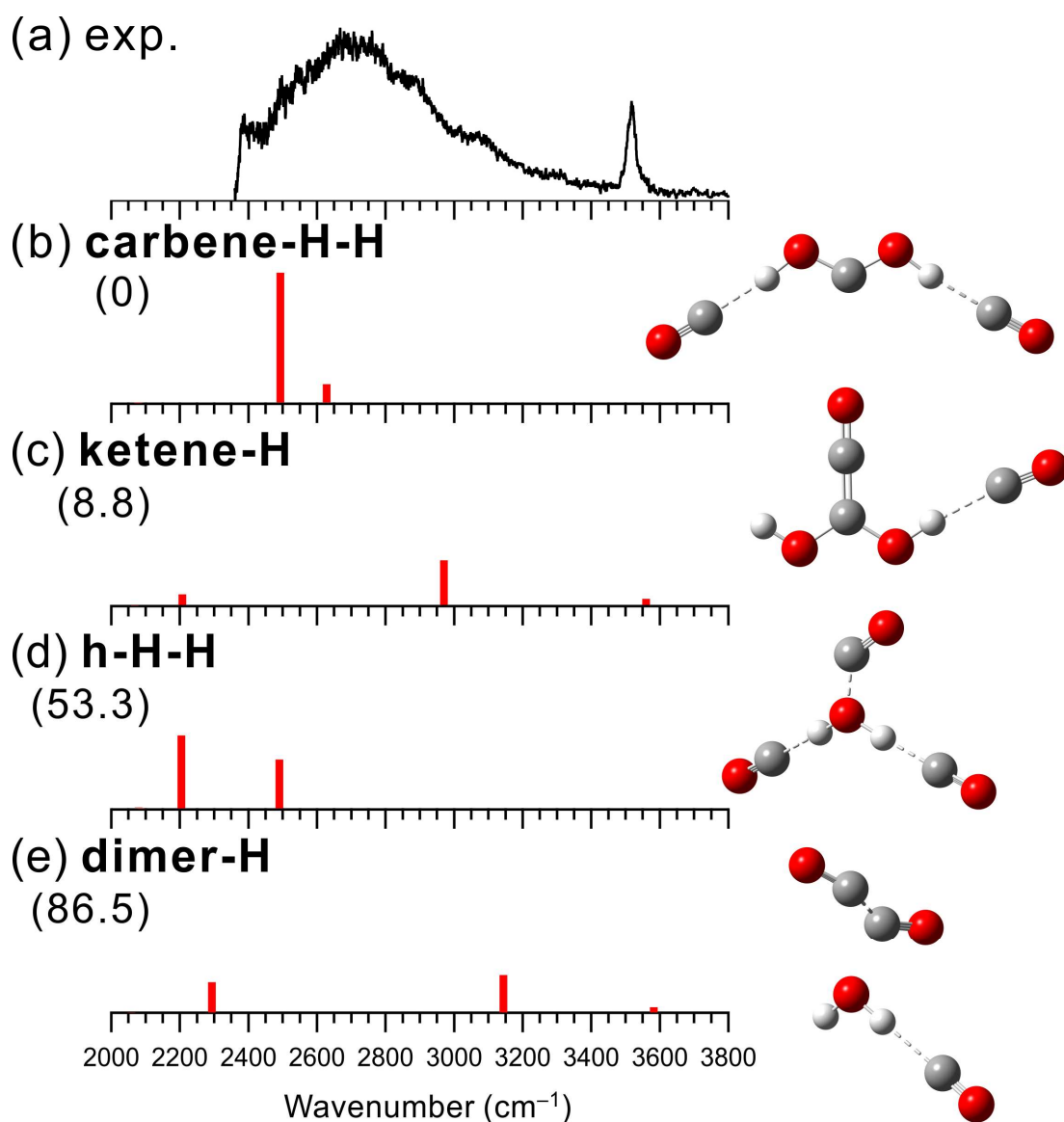


Fig. S11 Comparison of (a) observed IRPD spectrum of $[\text{H}_2\text{O}-(\text{CO})_3]^+$ and (b-e) simulated spectra of the stable isomers calculated at MP2/aug-cc-pVTZ. The simulated spectra were scaled by a factor of 0.955. The intensities of the simulated spectra of the isomers are plotted in the same scale. The schematic structures of the isomers are also shown. Numbers in parentheses are ZPE-corrected relative energies (in kJ/mol).

The broadened absorption around 2700 cm^{-1} in the observed spectrum can be attributed to CO-bound OH stretching vibrations. It should be noted that a peak is observed at 3520 cm^{-1} , which is attributed to a free OH stretching vibration. According to quantum chemical calculations, the most

stable structure is isomer **carbene-H-H**, of which both OH groups are H-bonded. However, since the free OH stretching band is observed, **carbene-H-H** alone cannot explain the observed spectrum. The contribution of either isomer **ketene-H** or **dimer-H** is plausible. However, it is difficult to uniquely determine which isomer is responsible for the observed free OH band.

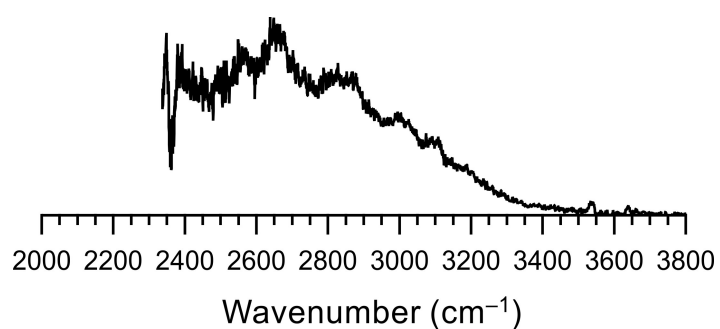


Fig. S12 Observed IRPD spectrum of $[\text{H}_2\text{O}-(\text{CO})_4]^+$. The heavily broadened absorption below 3400 cm^{-1} can be attributed to CO-bound OH stretching vibrations. It is noted that no free OH stretching band appears. For $n = 3$, stable isomers with one free OH are found (see Fig. S11). For $n = 4$, however, one more CO is added, and the free OH at $n = 3$ would be H-bonded to CO. Thus, the free OH band disappears in $n = 4$.

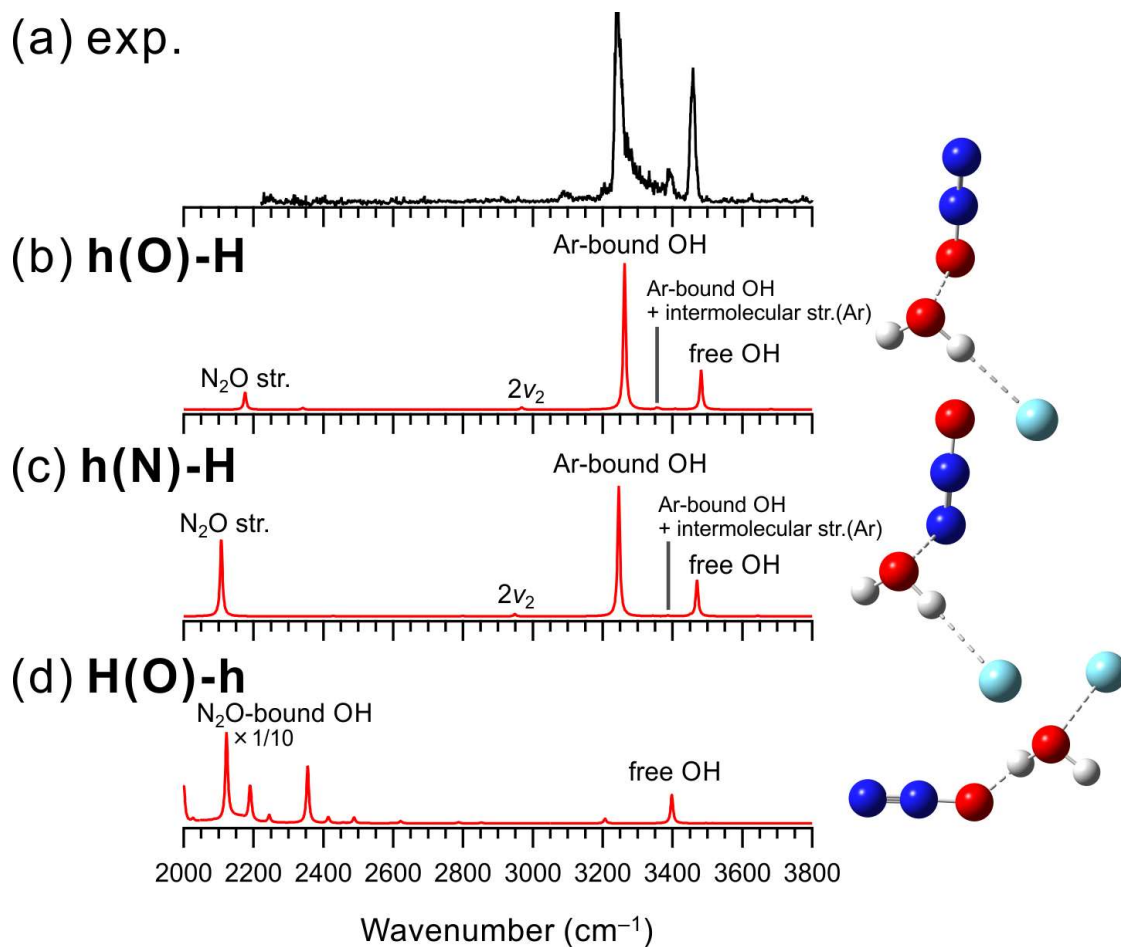


Fig. S13 Comparison of (a) observed IRPD spectrum of $[\text{H}_2\text{O}-\text{N}_2\text{O}]^+-\text{Ar}$ and (b-d) simulated anharmonic (VPT2) spectra of the stable isomers calculated at MPW2PLYPD/aug-cc-pVTZ. The intensities of the simulated spectra of the isomers are plotted in the same scale. The schematic structures of the isomers are also shown.

The peaks at 3240, 3390, and 3460 cm^{-1} in the observed spectrum can be attributed to the Ar-bound OH stretching, its combination band with the intermolecular stretching vibration, and free OH stretching vibration, respectively. In addition, the very weak peak at 3090 cm^{-1} could be the bending overtone of H_2O^+ . The anharmonic calculation results show that the hemibonded isomers (**h(O)-H** and **h(N)-H**) reproduce the main and minor features of the observed spectrum. Therefore, we conclude that the hemibond formation is preferred over the H-bond formation for $X = \text{N}_2\text{O}$. (see main text for details).

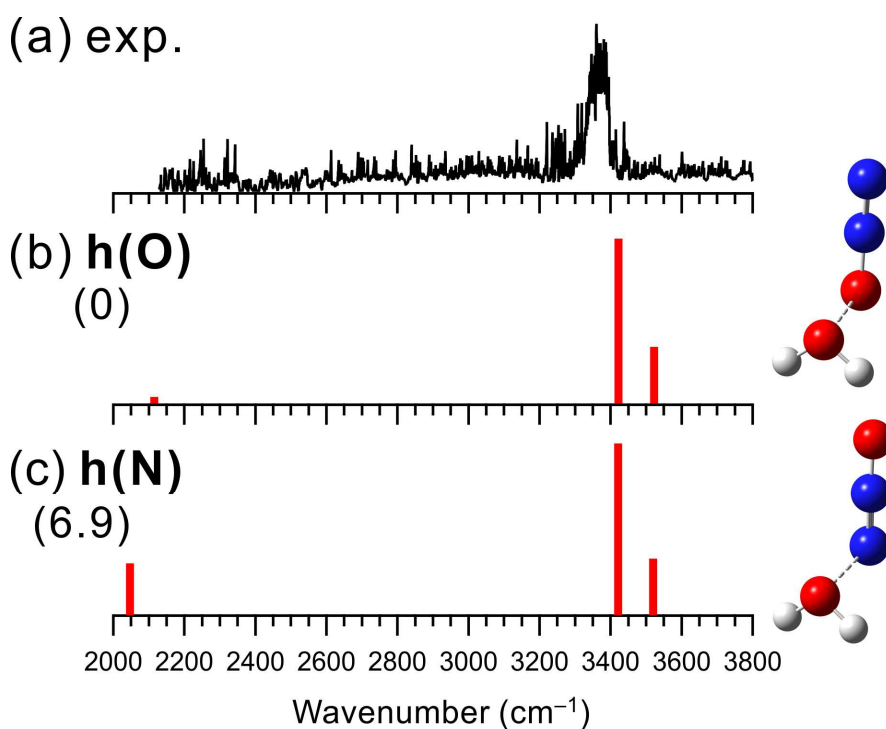


Fig. S14 Comparison of (a) observed IRPD spectrum of $[\text{H}_2\text{O}-\text{N}_2\text{O}]^+$ and (b, c) simulated spectra of the stable isomers calculated at B3LYP/aug-cc-pVTZ. The simulated spectra were scaled by a factor of 0.958. The intensities of the simulated spectra of the isomers are plotted in the same scale. The schematic structures of the isomers are also shown. Numbers in parentheses are ZPE-corrected relative energies (in kJ/mol).

The peak at 3370 cm^{-1} can be attributed to the free OH stretching vibrations of the H_2O^+ moiety. Only the hemibonded forms were obtained as stable structures, while the H-bonded form was calculated as a transition state. The O-bound isomer (**h(O)**) is more stable than the N-bound isomer (**h(N)**). These computational results are essentially the same as those at the B3LYP/6-311++G(d,p) level in the previous study by Matsushima *et al.*⁵ In their study, however, an experimental IR spectrum was not obtained.

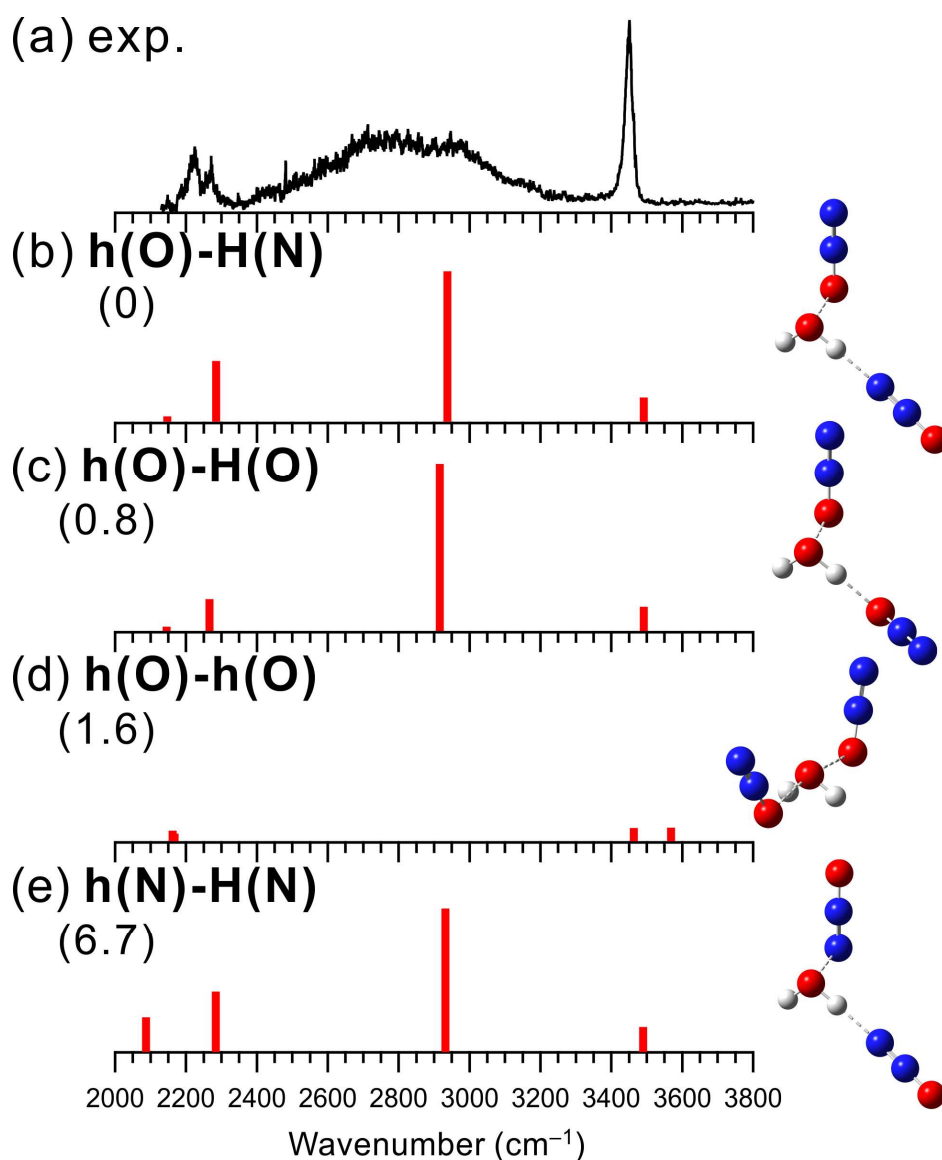


Fig. S15 Comparison of (a) observed IRPD spectrum of $[\text{H}_2\text{O}-(\text{N}_2\text{O})_2]^+$ and (b-e) simulated spectra of the stable isomers calculated at B3LYP/aug-cc-pVTZ. The simulated spectra were scaled by a factor of 0.958. The intensities of the simulated spectra of the isomers are plotted in the same scale. The schematic structures of the isomers are also shown. Numbers in parentheses are ZPE-corrected relative energies (in kJ/mol).

The bands around 2230, 2820, and 3450 cm^{-1} in the observed spectrum can be attributed to the N_2O stretching, the N_2O -bound OH stretching, and the free OH stretching vibrations, respectively. The appearance of the free OH stretching vibrational band demonstrates that the hemibond formation

is superior to the H-bond formation. Quantum chemical calculations also show that the hemibonded type isomers are more stable than the H-bonded type isomer (**H-H**, not shown in the figure) by more than 20 kJ/mol, supporting the experimental results. These experimental and theoretical results are essentially the same as those of the previous study by Matsushima *et al.*⁵

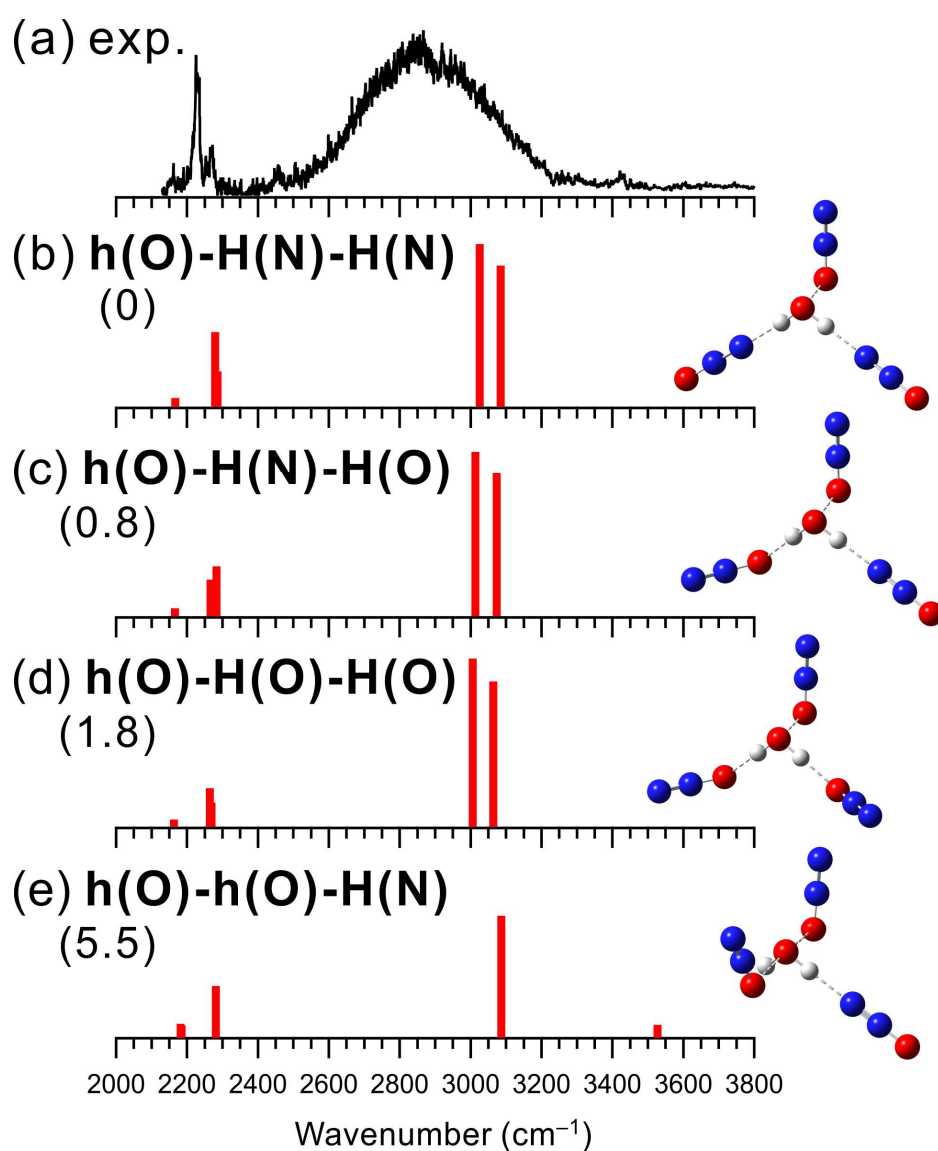


Fig. S16 Comparison of (a) observed IRPD spectrum of $[\text{H}_2\text{O}-(\text{N}_2\text{O})_3]^+$ and (b-e) simulated spectra of the stable isomers calculated at B3LYP/aug-cc-pVTZ. The simulated spectra were scaled by a factor of 0.958. The intensities of the simulated spectra of the isomers are plotted in the same scale. The schematic structures of the isomers are also shown. Numbers in parentheses are ZPE-corrected relative energies (in kJ/mol).

The bands around 2230 and 2870 cm^{-1} in the observed spectrum can be attributed to the N_2O stretching and the N_2O -bound OH stretching vibrations, respectively. No free OH stretch band is seen in the observed spectrum of $n = 3$. The observed spectrum is attributed to structures in which two

N₂O molecules are H-bonded to the OH groups and the third one is hemibonded to the O atom of H₂O⁺ (**h-H-H** isomers). The observed spectrum and the results of the theoretical computations are essentially the same as those of the previous study by Matsushima *et al.*⁵

References

- 1 J.-M. Liu, T. Nishigori, T. Maeyama, Q.-R. Huang, M. Katada, J.-L. Kuo and A. Fujii, *J. Phys. Chem. Lett.*, 2021, **12**, 7997–8002.
- 2 Y. Inokuchi, Y. Kobayashi, A. Muraoka, T. Nagata and T. Ebata, *J. Chem. Phys.*, 2009, **130**, 154304.
- 3 E. Uggerud, W. Koch and H. Schwarz, *Int. J. Mass Spectrom. Ion Process.*, 1986, **73**, 187–196.
- 4 C. Y. Wong, P. J. A. Ruttink, P. C. Burgers and J. K. Terlouw, *Chem. Phys. Lett.*, 2004, **390**, 176–180.
- 5 R. Matsushima, T. Ebata and Y. Inokuchi, *J. Phys. Chem. A*, 2010, **114**, 11037–11042.